Characterization of a Local Folding Event of the *Tetrahymena* Group I Ribozyme: Effects of Oligonucleotide Substrate Length, pH, and Temperature on the Two Substrate Binding Steps†

Geeta J. Narlikar,‡,§ Laura E. Bartley,|| Mala Khosla,|| and Daniel Herschlag*,‡,||

Departments of Chemistry and Biochemistry, Stanford University, Stanford, California 94305

Received June 22, 1999; Revised Manuscript Received August 26, 1999

ABSTRACT: Binding of the *Tetrahymena* group I ribozyme's oligonucleotide substrate occurs in two steps: P1 duplex formation with the ribozyme's internal guide sequence which forms an "open complex" is followed by docking of the P1 duplex into tertiary interactions within the catalytic core which forms a "closed complex". By systematically varying substrate length, pH, and temperature, we have identified conditions under which P1 duplex formation, P1 docking, or the chemical cleavage step limits the rate of the ribozyme reaction. This has enabled characterization of the individual steps as a function of substrate length, pH, and temperature, leading to several conclusions. (1) The rate constant for formation of the open complex is largely independent of substrate length, pH, and temperature, analogous to that of duplex formation in solution. This extends previous results suggesting that open complex formation entails mainly secondary structure formation and strengthens the view that the second binding step, P1 docking, represents a simple transition from secondary to tertiary structure in the context of an otherwise folded RNA. (2) The temperature dependence of the rate constant for P1 docking yields a negative activation entropy, in contrast to the positive entropy change previously observed for the docking equilibrium. This suggests a model in which tertiary interactions are not substantially formed in the transition state for P1 docking. (3) Shortening the substrate by three residues decreases the equilibrium constant for P1 docking by 200-fold, suggesting that the rigidity imposed by full-length duplex formation facilitates formation of tertiary interactions. (4) Once docked, shortened substrates are cleaved at rates within 3-fold of that for the full-length substrate. Thus, all the active site interactions required to accelerate the chemical cleavage event are maintained with shorter substrates. (5) The rate constant of $\sim 10^3$ min^{-1} obtained for P1 docking is significantly faster than the other steps previously identified in the tertiary folding of this RNA. Nevertheless, P1 docking presumably follows other tertiary folding steps because the P1 duplex docks into a core that is formed only upon folding of the rest of the ribozyme.

The *Tetrahymena* group I ribozyme provides an attractive system for investigating the principles of RNA folding. Phylogenetic and biochemical analyses have determined the secondary structure of this ribozyme and have also led to a model for the tertiary structure (*1*−*3*). This model has been supported and refined by biochemical studies, mutagenesis, the recently solved 2.8 Å crystal structure of the P4−P6 domain, and the lower-resolution X-ray data obtained for the catalytic core (*4*−*18*). Further, the ribozyme's well-characterized catalytic activity provides a direct readout for the correct functional structure (*9*, *19*−*29*).

Substantial previous work has led to a minimal model for the tertiary folding of the *Tetrahymena* ribozyme in which folding proceeds via formation of a series of substructures (Figure 1) (*9*, *10*, *15*, *30*−*33*). Formation of the P5abc region stabilizes folding of the P4−P6 domain, which in turn stabilizes folding of the P3−P7 domain. Each step entails the folding of large regions of the ribozyme and results in formation of complex tertiary structures. This makes it difficult to carry out detailed studies of these tertiary folding steps. To study RNA tertiary folding in detail, we have characterized a smaller, more localized folding step in which the P1 duplex, formed between the ribozyme's oligonucleotide substrate (S)[1] and its internal guide sequence (IGS), docks into tertiary interactions within an otherwise folded core [Figures 1 and 2 (*12*, *14*, *15*, *20*, *25*, *34*−*41*)].

The docking step was isolated in this study by shortening the substrate and varying the pH and temperature such that P1 docking limits the rate of the ribozyme-catalyzed reaction. The effects of substrate length, pH, and temperature on the identity of the rate-limiting step have allowed characterization of P1 docking as well as P1 duplex formation and the chemical cleavage step (Figure 2A). The results strengthen the previous view that P1 docking represents a simple transition between secondary and tertiary structure and provide additional information about the nature of the docking step.

† This work was supported by NIH Grant GM49243 to D.H.

* To whom correspondence should be addressed: Department of Biochemistry, B400 Beckman Center, Stanford University, Stanford, CA 94305-5307. Phone: (650) 723-9442. Fax: (650) 723-6783. E-mail: herschla@cmgm.stanford.edu.

‡ Department of Chemistry, Stanford University.

§ Present address: Department of Molecular Biology, Massachusetts General Hospital, Boston, Massachusetts 02114.

|| Department of Biochemistry, Stanford University.

10.1021/bi9914309 CCC: $18.00
Published on Web 10/08/1999

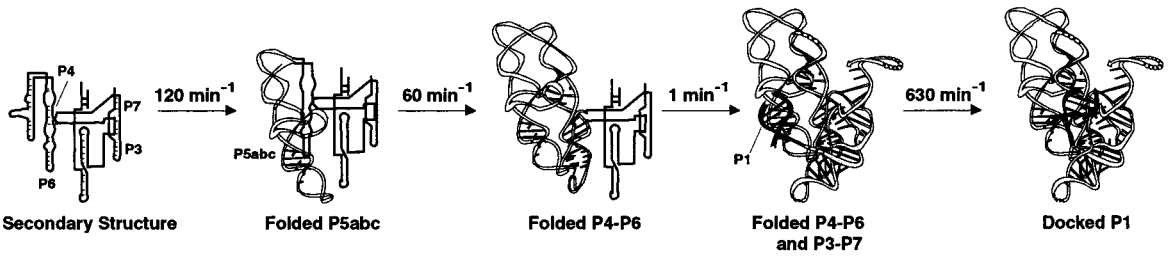

FIGURE 1: Steps involved in the overall tertiary folding of the ribozyme (*9*, *10*, *15*, *30*−*33*). The last step involves docking of the P1 duplex into the catalytic core formed by P4−P6 and P3−P7 (see the Discussion). The rate constants are for ~40 °C, 10 mM $MgCl_2$, and pH 7. The values for P5abc, P4−P6, and P3−P7 folding are from previous work (*32*, *33*), and the rate constant for P1 docking is from Table 3. The nonconserved peripheral elements P2, P2.1, P9, P9.1, and P9.2 are not shown for clarity.

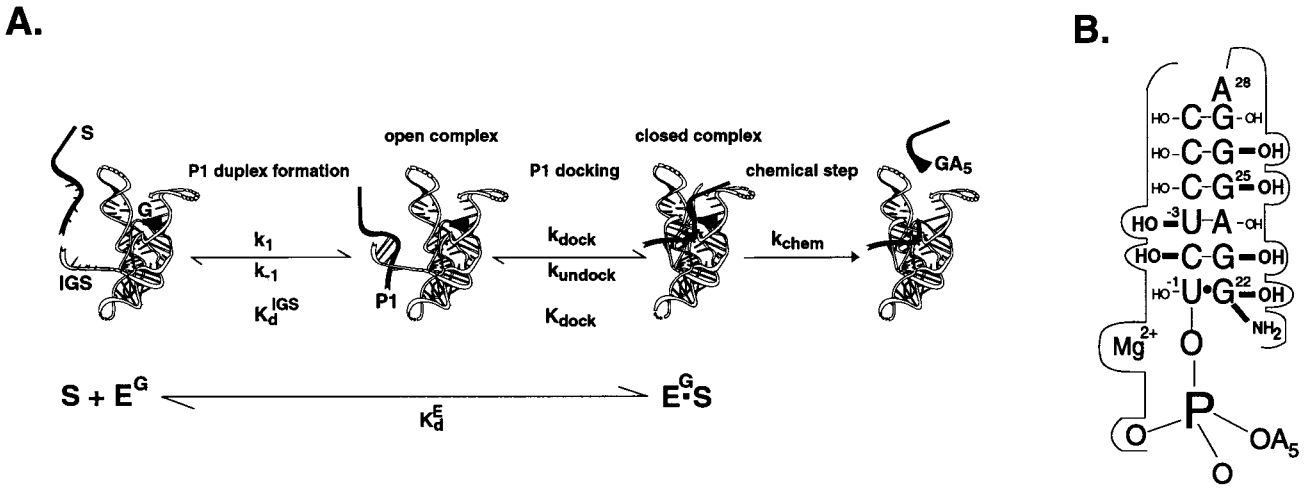

FIGURE 2: Binding of the oligonucleotide substrate. (A) The oligonucleotide substrate binds in two steps prior to catalytic cleavage (*14*, *20*, *25*, *74*). The substrate (S) first base pairs with the internal guide sequence (IGS) of the ribozyme to form the P1 duplex in the open complex. The P1 duplex then docks into the catalytic core via specific tertiary interactions to give a closed complex. The docked substrate is cleaved by a bound exogenous guanosine molecule (G). K_d^E is the observed equilibrium constant for dissociation of S from the $E^G{\cdot}S$ complex; K_d^{IGS} is the equilibrium constant for dissociation of S from the open complex, and K_{dock} is the equilibrium constant for docking into the tertiary interactions. As in Figure 1, several structural elements are omitted for clarity. (B) The oligonucleotide substrate is held by both base pairing interactions with the internal guide sequence of the ribozyme (IGS ≡ 5′-GGAGGG) as well as tertiary interactions (*12*, *24*, *34*−*41*). The ribozyme active site is represented schematically by the outline. The 2′-OH groups shown explicitly and the exocyclic amino group of the G·U wobble pair shown in bold stabilize the tertiary structure of the P1 duplex.

MATERIALS AND METHODS

Materials. The L-21 *ScaI Tetrahymena* ribozyme (E) was prepared by in vitro transcription and purified as described previously (*42*). Oligonucleotides were made by solid-phase synthesis (*43*). Several were supplied by CloneTec (Palo Alto, CA) or by the Protein and Nucleic Acid Facility at Stanford or were used and characterized in previous studies. Phosphorothioate substrates were applied to a Dionex Nucleo Pac PA-100 anion exchange HPLC column to purify the R_P-stereoisomer. Separation of the R_P- and S_P-stereoisomers from contaminating non-thio substrates was achieved using a linear gradient of 167 to 265 mM NaCl in 10 mM Tris (pH 8.0) and 10% ethanol at a flow rate of 5 mL/min over the course of 40 min. Stereoisomers were assigned from relative reactivity, on the basis of previous results (*44*−*46*). Oligonucleotide substrates were 5′-end labeled with approximately equimolar amounts of [γ-^{32}P]ATP using T4 polynucleotide kinase, and purified by nondenaturing polyacrylamide gel electrophoresis, as described previously (*36*).

General Kinetic Methods. All reactions were carried out in the presence of 10 mM $MgCl_2$ and 50 mM buffer as described previously (*19*, *36*). The buffers used in the reactions and their pH values at 25 °C were as follows: sodium MES, pH 5.2−6.8; sodium MOPS, pH 6.5−7.3; and sodium EPPS, pH 7.2. Unless otherwise noted, pH values are corrected for the temperature of the reactions (*47*, *48*). pH values beyond this range were not used because ribozyme activity decreases below pH 5 and above pH 7.5, presumably due to multiple protonations and deprotonations, respectively, of ribozyme functional groups (*48*). Temperatures higher than 65 °C were not used because previous work suggests that the ribozyme's tertiary structure is mostly disrupted above this temperature (*30*).

[1] Abbreviations: E, *Tetrahymena* L-21 *Sca*I group I ribozyme; G, guanosine; S, oligonucleotide substrate without specification of length or sugar identity; S*, ^{32}P-5′-end-labeled oligonucleotide substrate; IGS, ribozyme's internal guide sequence, 5′-GGAGGG; 5′-pyr, 5′-pyrene group; MES, 2-(*N*-morpholino)ethanesulfonic acid; MOPS, 2-(*N*-morpholino)propanesulfonic acid; EPPS, *N*-(2-hydroxyethyl)piperazine-*N*′-3-propanesulfonic acid; EDTA, (ethylenedinitrilo)tetraacetic acid; Tris, tris(hydroxymethyl)aminomethane. The sequences of the shorter substrates are represented with the missing bases replaced with a hyphen. Thus, - -CUCUA$_5$ represents a substrate that is two bases shorter than the full-length substrate, CCCUCUA$_5$. mU refers to a 2′-methoxy substituent and dU to a 2′-deoxy substituent at a U residue. Thus, CCCmUCUA$_5$ refers to a substrate with a 2′-methoxy-2′-deoxyribose residue at position −3 (positions defined in Figure 2B) and ribose residues at all other positions. Similarly, CCCUCdUA$_5$ refers to a substrate with a 2′-deoxyribose residue at position −1 and ribose residues at all other positions.

Reactions at 50 °C were initiated by addition of 5′-end-labeled substrate, S*, following a 15 min, 50 °C preincubation of E in 10 mM $MgCl_2$ and buffer. Reactions at all other temperatures were initiated after a 30 min, 50 °C preincubation followed by a ~5 min incubation at the temperature of reaction (*39*). Six aliquots (1−2 μL) were removed from 20 μL reaction mixtures at specified times, and further reaction was quenched by the addition of ~2 volumes of 20 mM EDTA in 90% formamide with 0.005% xylene cyanol, 0.01% bromophenol blue, and 1 mM Tris (pH 8). Substrate and product(s) were separated by electrophoresis on 20% polyacrylamide/7 M urea gels, and their ratio at each time point was quantitated with a Molecular Dynamics PhosphorImager.

All reactions were single-turnover except for those used in the determination of k_{chem} for - - -$UCUA_5$. Single-turnover reactions were carried out with E (5−1000 nM) in excess of S* (0.01−0.05 nM) and were typically followed for about three half-times ($t_{1/2}$). The slow reactions of - -$CUCUA_5$ and - - -$UCUA_5$ at temperatures above 55 °C and of - -$CU\underline{C}\underline{dU}A_5$ at 50 °C and pH 5 were followed only to 10% reaction because ribozyme activity decreases after longer periods of time. End points of 85−95% were obtained at the different temperatures and were used in nonlinear least-squares fits to the data to determine the first-order rate constant for the disappearance of S* (KaleidaGraph, Synergy Software, Reading, PA). Reactions for which only initial rates could be measured were assumed to have the same end points as faster reactions at the same temperature; several results from previous work suggest that the reaction end points are not significantly affected by substrate identity or pH and are affected slightly by changes in temperature (*19*, *39*; G. J. Narlikar and D. Herschlag, unpublished results). Multiple-turnover reaction mixtures contained unlabeled - - -$UCUA_5$ (80−480 μM) with trace amounts of 5′-end-labeled - - -$UCUA_5$ (0.01−0.05 nM) in excess of E (0.5 μM). Rate constants for these reactions were determined from initial rates obtained from linear least-squares fits to data from the first 10% of the reaction.

Determination of Rate Constants. The observed rate constant for a given single-turnover reaction is termed k_{obs}. $(k_{cat}/K_m)^S$ represents the second-order rate constant for the reaction $E^G + S \rightarrow$ products. k_{chem} is the rate constant for reaction from the E^G·S closed complex (Figure 2A). Under "$(k_{cat}/K_m)^S$ conditions", most of S is not bound to E^G and k_{obs} is linearly proportional to the concentration of E with a slope that equals $(k_{cat}/K_m)^S$. At least three concentrations of E were used for each $(k_{cat}/K_m)^S$ determination. Thio effects were calculated from the ratio of k_{obs} values for the normal and corresponding phosphorothioate substrate and were measured in triplicate. The k_{chem} value for $CCCUC\underline{dU}A_5$ in Table 4 was obtained from k_{obs} measured with saturating concentrations of E and G at 50 °C and pH 6.6; $CCCUC\underline{d}\underline{U}A_5$ is predominantly docked under these conditions (*36*, *41*). The k_{chem} values for $CCCUCUA_5$, -$CCUCUA_5$, and - -$CUCUA_5$ listed in Table 5 were determined from k_{obs} values measured using saturating concentrations of E and G at 10 °C and pH 6.3 or 5.4. Saturation by E was confirmed by the observation that the rate was unaffected by a 5-fold variation in the concentration of E. The k_{chem} value for - - -$UCUA_5$ was estimated from the k_{cat} value measured using saturating - - -$UCUA_5$ in multiple-turnover reactions. Saturation by - - -$UCUA_5$ was confirmed by the observation that the rate was unaffected by a ~6-fold variation in the concentration of - - -$UCUA_5$. Previous data suggest that $CCCUCUA_5$, -$CCUCUA_5$, and - -$CUCUA_5$ are docked at 10 °C (see the Results). - - -$UCUA_5$ may not be stably docked at 10 °C, so the reported k_{chem} value for - - -$UCUA_5$ is a lower limit (see the Results).

Determination of K_d^{IGS}, the Dissociation Constant of the Open Complex. The value of K_d^{IGS} (Figure 2A) for a given oligonucleotide substrate was estimated from the equilibrium dissociation constant of E·S, K_d^E, for a substrate analogue having a 2′-methoxy substituent at the −3 position (Figure 2B). Previous structural and thermodynamic results have provided strong evidence that substrates with 2′-methoxy substituents at the −3 position bind predominantly in the open complex (*39*, *49*). In addition, in high concentrations of Na^+, which cause the all-RNA substrate, CCCUCUA, to bind predominantly in the open complex, the E·S complex formed with CCCUCUA has the same stability as that formed with $CCC\underline{mU}CUA$ [K_d^E(CCCUCUA) = 640 nM and K_d^E($CCC\underline{mU}CUA$) = 990 nM at 50 °C, and K_d^E(CCCUCUA) = 2.8 nM and K_d^E($CCC\underline{mU}CUA$) = 2.6 nM at 30 °C (pH 6.1, 10 mM Mg^{2+}, and 1.6 M Na^+) (ref *49* and data not shown)]. These results suggest that the 2′-methoxy substituent prevents docking but does not alter the stability of the open complex so that the E·S complex formed with the modified substrate serves as a good mimic of the open complex formed with the all-RNA substrate.

The K_d^{IGS} values for $CCCUCUA_5$ at different temperatures and pH 6.8 (pH value at 25 °C) were calculated from the temperature dependence of K_d^E for $CCC\underline{mU}CUA_5$ between 30 and 60 °C, which is described by $\Delta H = -45.1$ kcal/mol and $\Delta S = -108$ cal mol^{-1} K^{-1} (data not shown). The K_d^{IGS} values for -$CCUCUA_5$ and - -$CUCUA_5$ were analogously obtained from the temperature dependence of K_d^E for -$CC\underline{mU}CUA_5$ between 10 and 50 °C ($\Delta H = -37.2$ kcal/mol and $\Delta S = -90$ cal mol^{-1} K^{-1}) and of K_d^E for - -$C\underline{mU}CUA_5$ between 0 and 20 °C ($\Delta H = -26.7$ kcal/mol and $\Delta S = -65$ cal mol^{-1} K^{-1}), respectively (data not shown). For each substrate, values of K_d^{IGS} at temperatures beyond the measured range were obtained by extrapolation from the respective temperature dependence. The K_d^{IGS} value for - - -$UCUA_5$ was obtained from the K_d^{IGS} value for - -$CUCUA_5$ using nearest-neighbors rules for the destabilizing effect of removing the terminal G·C base pair adjacent to the A·U base pair (*50*). This approximation was necessary because of the weaker binding of - - -$\underline{mU}CUA_5$ compared to that of the other substrates.

The K_d^{IGS} values for $CCCUC\underline{dU}A_5$, -$CCUC\underline{dU}A_5$, and - -$CUC\underline{dU}A_5$ listed in Table 4 were obtained from the K_d^{IGS} values for the corresponding all-RNA substrates by correcting for a 3-fold destabilizing effect of the 2′-deoxyribose substitution on the stability of the P1 duplex. This destabilizing effect is obtained from the 3-fold destabilizing effect of the corresponding 2′-deoxyribose substitution in a full-length model P1 duplex under the same conditions (pH 6.6, 50 °C, and 10 mM $MgCl_2$) (*41*) and the expected independence of this effect from removal of remote base pairs (*24*, *41*, *50*, *51*).

The K_d^E values of the 2′-methoxy-substituted substrates were obtained from a dependence of the rate constant for S

cleavage on the concentration of E as described previously (*39*, *49*). Control experiments indicated that each concentration dependence reflects the true equilibrium dissociation constant, K_d^E (*22*, *39*).

Determination of $\Delta H^{\ddagger}_{dock}$ and $\Delta S^{\ddagger}_{dock}$ from Arrhenius Plots. The lines in Figure 8 are fits to the Arrhenius equation (eq 1) in which k_B is the Boltzmann constant, h is Planck's constant, R equals 0.00198 kcal mol^{-1} K^{-1}, and T is the temperature in kelvin.

$$\ln(k_{dock}) = \ln(A) - E/RT; \quad A = (ek_BT/h)\exp(\Delta S^{\ddagger}_{dock}/R); \quad E = \Delta H^{\ddagger}_{dock} + RT \quad (1)$$

The value of $\Delta H^{\ddagger}_{dock}$ is obtained from the slope, E/R, and that of $\Delta S^{\ddagger}_{dock}$ from the intercept, ln(A), using a T of 323 K (50 °C).

Estimation of Errors. Rate constants varied typically by ±20% in independent experiments. Thio effects typically varied by ±10% in independent experiments. The K_d^E values for the substrates modified with 2′-methoxy substitutions typically varied by ±15% so that the K_d^{IGS} values obtained from these K_d^E values were also estimated to vary by ±15%. The values of k_{dock} were calculated from K_d^{IGS} and $(k_{cat}/K_m)^S$ values (eq 4), so the error limits for k_{dock} were conservatively estimated as the sum of the error limits for the K_d^{IGS} and $(k_{cat}/K_m)^S$ values, i.e., ±35% (~2-fold variation). Analogous conservative error limits of ±55% were obtained for K_{dock}, which is calculated from K_d^{IGS} (±15%), $(k_{cat}/K_m)^S$ (±20%), and k_{chem} (±20%) using eq 6.

$\Delta S^{\ddagger}$ values are particularly sensitive to small experimental variations in the individual rate constants because the intercept of the Arrhenius plot, which is used to determine $\Delta S^{\ddagger}$ (eq 1), is obtained from a long extrapolation to infinite temperature ($1/T = 0$ in Figure 8). The intercept is most sensitive to variations of rate constants at the extremes of the temperature range. To determine whether the sign of $\Delta S^{\ddagger}_{dock}$ remains the same with experimental variations in k_{dock}, highly conservative upper and lower limits for $\Delta H^{\ddagger}_{dock}$ and $\Delta S^{\ddagger}_{dock}$ were obtained by varying the k_{dock} values at the temperature extremes by 2-fold (±35%) and then fitting the varied values to eq 1; i.e., the k_{dock} value at 30 °C was decreased 2-fold, and that at 60 °C was increased 2-fold and vice versa. Error limits of ±10 kcal/mol and ±27 cal mol^{-1} K^{-1} were calculated for $\Delta H^{\ddagger}_{dock}$ and $\Delta S^{\ddagger}_{dock}$, respectively. The maximum value of $\Delta S^{\ddagger}_{dock}$ specified by the error limits (−10 cal mol^{-1} K^{-1}) is still negative, suggesting that although there may be substantial error in the magnitude of $\Delta S^{\ddagger}_{dock}$, the sign of $\Delta S^{\ddagger}_{dock}$ is not affected by experimental variations in k_{dock}.

Construction of Free Energy Reaction Profiles. Each free energy profile in Figures 5−7 schematically depicts the activation energy barriers associated with P1 duplex formation and dissociation, P1 docking and undocking, and the chemical step. These figures are presented to facilitate interpretation of and to summarize the data. The free energy differences in the figures have been exaggerated for clarity in a manner that does not change the conclusions obtained from a comparison of the actual free energy barriers, which were derived as follows. The activation free energy, $\Delta G^{\ddagger}$, for each step is related to the rate constant for the step, k, according to eq 2, in which k_B is the Boltzmann constant, h is Planck's constant, R equals 0.00198 kcal mol^{-1} K^{-1}, and T is the temperature in kelvin.

$$\Delta G^{\ddagger} = -RT\ln(hk/k_BT) \quad (2)$$

Table 1: Effect of Substrate Length on $(k_{cat}/K_m)^S$ [a]

substrate	$(k_{cat}/K_m)^S$ [b] (M^{-1} min^{-1})	$1/(k_{cat}/K_m)^{S,rel}$ [c]
CCCUCUA$_5$	1.8×10^8	(1)
-CCUCUA$_5$	1.4×10^8	1.3
- -CUCUA$_5$	7.1×10^6	25
- - -UCUA$_5$	2.9×10^4	6200

[a] Conditions: 50 °C, 50 mM sodium MES, pH 6.6, and 10 mM $MgCl_2$. [b] $(k_{cat}/K_m)^S$ is the second-order rate constant for the reaction $E^G + S \rightarrow$ products and was obtained as described in Materials and Methods. Each $(k_{cat}/K_m)^S$ value is the average of two determinations. [c] $(k_{cat}/K_m)^{S,rel} = [(k_{cat}/K_m)^S]^{short-S}/[(k_{cat}/K_m)^S]^{full-length-S}$ so that $1/(k_{cat}/K_m)^{S,rel}$ represents the amount the reaction is slowed relative to the rate of the full-length substrate.

The reaction profiles were constructed for a standard state of 1 pM E, which is subsaturating for all substrates and temperatures used, [S] ≪ [E], and a saturating G concentration. The rate and equilibrium constants for each step are defined in Figure 2A. The results used and assumptions made to obtain the individual rate and equilibrium constants are noted below.

For each reaction profile, the value of k_1 was taken to be 1.8×10^8 M^{-1} min^{-1}, the $(k_{cat}/K_m)^S$ value for the full-length substrate at 50 °C and pH 6.6 reported in Table 1. This assumption is based on previous results and results herein, which suggest that P1 duplex formation limits $(k_{cat}/K_m)^S$ for CCCUCUA$_5$ and that k_1 is essentially independent of substrate length, pH, and temperature (see the Results). For each substrate, the K_d^{IGS} value at a given temperature and pH 6.8 was obtained as described in Determination of K_d^{IGS}, the Dissociation Constant of the Open Complex. K_d^{IGS} was assumed to be independent of pH on the basis of the pH independence of the stability of a model P1 duplex in solution between pH 5 and 7 (*41*) and the pH independence of K_d^{IGS} for the full-length substrate between pH 5.9 and 6.6 (*49*). The value of k_{-1} was derived from the K_d^{IGS} and k_1 values using the equation $k_{-1} = K_d^{IGS}k_1$.

The k_{dock} values for CCCUCUA$_5$ and -CCUCUA$_5$ at different temperatures were assumed to be the same as that for - -CUCUA$_5$ reported in Table 3. This is a simple, though untested, extrapolation of the results herein, which suggest that at 65 °C k_{dock} is the same, within error, for - -CUCUA$_5$ and -CCUCUA$_5$. Analogously, K_{dock} values were assumed to be the same for CCCUCUA$_5$, -CCUCUA$_5$, and - -CUCUA$_5$ at all temperatures based on the data in Table 4, which suggests that K_{dock} is the same for these substrates at 50 °C (Table 4). The previously determined temperature dependence of K_{dock} for the full-length substrate was then used to obtain K_{dock} values for CCCUCUA$_5$, -CCUCUA$_5$, and - -CUCUA$_5$ at a given temperature (*49*). For - - -UCUA$_5$, K_{dock} is significantly smaller than for the longer substrates (Table 4), suggesting that k_{dock} may also differ. Hence, for - - -UCUA$_5$, k_{undock} and k_{dock} were not explicitly assigned. For CCCUCUA$_5$, -CCUCUA$_5$, and - -CUCUA$_5$, the value of k_{undock} was derived from the K_{dock} and k_{dock} values using the equation $k_{undock} = k_{dock}/K_{dock}$.

The k_{chem} value for each substrate was assumed to be the same as that for the full-length substrate on the basis of the

results listed in Table 5, which suggest that k_{chem} is similar for all the substrates at 10 °C. The previously determined pH and temperature dependencies of k_{chem} for the full-length substrate (*21*−*23*, *48*) were used to obtain k_{chem} at each pH and temperature.

RESULTS

The standard oligonucleotide substrate of the *Tetrahymena* group I ribozyme (E), $CCCUCUA_5$, forms six base pairs with the ribozyme's internal guide sequence (IGS), GGAGGG; this duplex is termed the P1 duplex (Figure 2B). Table 1 summarizes the effect of shortening the oligonucleotide substrate on the kinetic parameter $(k_{cat}/K_m)^S$, which represents the observed second-order rate constant for the reaction of the oligonucleotide substrates (S) with the E^G binary complex (eq 3).

$$E^G + S \xrightarrow{(k_{cat}/K_m)^S} \text{products} \qquad (3)$$

Shortening the oligonucleotide substrate by one residue to give $-CCUCUA_5$ does not affect $(k_{cat}/K_m)^S$, whereas shortening the substrate by two residues ($- -CUCUA_5$) and three residues ($- - -UCUA_5$) slows the reaction 25- and 6200-fold, respectively.

Previous studies have identified three individual steps in the single-turnover reaction of oligonucleotide substrates with E^G: two binding steps and the chemical step (Figure 2A; *19*, *20*, *25*, *26*). The first binding step entails P1 duplex formation between the substrate and the IGS which gives the open complex, and the second binding step entails docking of this duplex into tertiary interactions with the ribozyme core which gives a closed complex (Figure 2; *12*, *14*, *15*, *20*, *25*, *34*−*41*). The chemical step includes a deprotonation step in addition to chemical cleavage of the substrate and any associated conformational changes of the closed complex (*21*, *48*, *52*). Interpretation of the effects of shortening the substrate requires identifying which individual step limits the rate of reaction. The first section of the Results describes the identification of the rate-limiting step for each oligonucleotide substrate using the framework of three individual steps described above. Results from this section are then used and expanded in the second section to obtain information about the nature of the individual reaction steps.

Identifying the Rate-Limiting Step for the Reaction of the Oligonucleotide Substrates of Varying Length

P1 Duplex Formation Is Rate-Limiting for the Reaction of $CCCUCUA_5$ and $-CCUCUA_5$. Previous results suggest that P1 duplex formation limits the rate of reaction of the full-length substrate with E^G as summarized below. (i) A transiently formed ribozyme•oligonucleotide complex having the same stability as a model P1 duplex was detected using the fluorescent changes accompanying the binding of 5′-pyrene-labeled - -CUCU (*25*). The rate constant for formation of this complex is the same as the $(k_{cat}/K_m)^S$ value for $CCCUCUA_5$, consistent with P1 duplex formation limiting $(k_{cat}/K_m)^S$ for $CCCUCUA_5$ (*19*, *25*). (ii) The chemical step was previously identified on the basis of its log-linear pH dependence and its sensitivity to substitution of the cleavage site *pro*-R_P phosphoryl oxygen with a sulfur (*21*, *46*, *48*). The absence of a pH dependence and thio effect for $(k_{cat}/K_m)^S$ suggested that a step other than chemical cleavage was rate-limiting (*46*; D. S. Knitt and D. Herschlag, unpublished results and see below). (iii) The $(k_{cat}/K_m)^S$ value for mutant ribozymes and oligonucleotide substrates that have reduced levels of tertiary stabilization was observed to be the same as that for reaction of the wild-type ribozyme with $CCCUCUA_5$ (*20*, *36*, *37*, *53*), consistent with rate-limiting duplex formation. (iv) With ribozymes having mutations in the J1/2 region that joins the IGS to the rest of the ribozyme, substitution of the *pro*-R_P phosphoryl oxygen with a sulfur at the correct cleavage site does not affect $(k_{cat}/K_m)^S$ but does reduce the ratio of correct to incorrect cleavage products (*20*, *53*). Incorrect cleavage occurs when the P1 duplex docks into an alternative tertiary binding register. Hence, these results suggested that the choice of the docking register and cleavage site is made after rate-limiting P1 duplex formation. Further, processive substrate cleavage by one of the mutant ribozymes demonstrated that the P1 duplex can undock from the correct register and dock into alternative registers without dissociation of the substrate from the P1 duplex. These results indicated that even with weakened docking, the barrier for dissociation of the substrate from the P1 duplex is greater than the barrier for P1 docking, thus providing strong evidence that P1 duplex formation is rate-limiting (*20*).

Under the standard conditions, the value of $(k_{cat}/K_m)^S$ for $-CCUCUA_5$ is the same, within error, as that for the full-length substrate, $CCCUCUA_5$, suggesting that P1 duplex formation also limits the reaction of $-CCUCUA_5$ (Table 1). This conclusion is supported by the results depicted in Figures 3 and 4, which show that $(k_{cat}/K_m)^S$ is the same for these substrates over a range of pHs and temperatures. The smaller values of $(k_{cat}/K_m)^S$ for $- -CUCUA_5$ and $- - -UCUA_5$ (Table 1) suggest that if P1 duplex formation limits the reaction of these substrates, the rate constant for P1 duplex formation is smaller for $- -CUCUA_5$ and $- - -UCUA_5$ than for $CCCUCUA_5$. Alternatively, P1 docking or the chemical step limits the rate for $- -CUCUA_5$ and $- - -UCUA_5$. We first tested whether the chemical step was rate-limiting for reaction of $- -CUCUA_5$ and $- - -UCUA_5$.

pH Dependence and Thio Effects Distinguish Rate-Limiting Chemical Cleavage from Rate-Limiting P1 Duplex Formation and Docking. Previous work has suggested that the chemical step of the *Tetrahymena* ribozyme reaction has a log-linear pH dependence with a slope of 1 between pH 5 and 7 (*21*, *48*). In contrast, under conditions of rate-limiting P1 duplex formation (see above), $(k_{cat}/K_m)^S$ for $CCCUCUA_5$ is independent of pH over this range (D. S. Knitt and D. Herschlag, unpublished results). The equilibrium constant for docking is largely independent of pH between 5 and 7 so that the rate constant for P1 docking is also expected to be pH-independent (*41*; G. J. Narlikar and D. Herschlag, unpublished results). Hence, to distinguish between rate-limiting chemical cleavage and rate-limiting duplex formation and docking, the dependence of $(k_{cat}/K_m)^S$ on pH was determined.

As shown in Figure 3, the value of $(k_{cat}/K_m)^S$ for $-CCUCUA_5$ is independent of pH between 5 and 7, analogous to the behavior of $CCCUCUA_5$. This is consistent with the above conclusion that P1 duplex formation limits the rate for $-CCUCUA_5$. In contrast, $(k_{cat}/K_m)^S$ for $- - -UCUA_5$ shows a log-linear pH dependence with a slope of 1 over this pH range, suggesting that the reaction of $- - -UCUA_5$ is limited

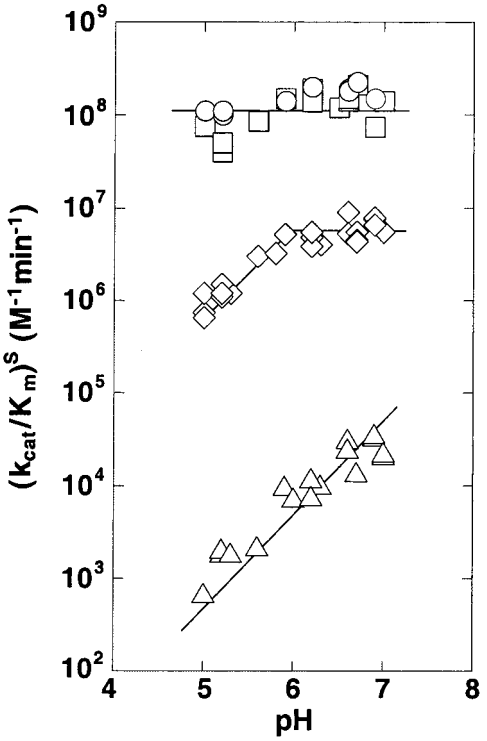

FIGURE 3: Effect of pH on $(k_{cat}/K_m)^S$ for the reaction of $CCCUCUA_5$ (○), -$CCUCUA_5$ (□), - -$CUCUA_5$ (◇), and - - -$UCUA_5$ (△) (50 °C, 10 mM $MgCl_2$, and 50 mM buffer). The line drawn through the $(k_{cat}/K_m)^S$ values for - - -$UCUA_5$ has a slope of 1, and the line drawn through the $(k_{cat}/K_m)^S$ values for $CCCUCUA_5$ and -$CCUCUA_5$ has a slope of 0. The line drawn through the $(k_{cat}/K_m)^S$ values for - -$CUCUA_5$ has a slope of 1 between pH 5.0 and 5.8 and a slope of 0 between pH 5.8 and 7.

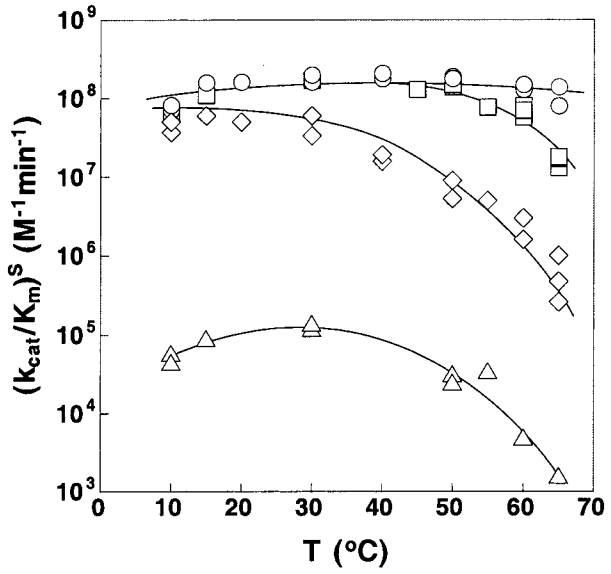

FIGURE 4: Effect of temperature on $(k_{cat}/K_m)^S$ for the reaction of $CCCUCUA_5$ (○), -$CCUCUA_5$ (□), - -$CUCUA_5$ (◇), and - - -$UCUA_5$ (△) (sodium MES, pH 6.8, at 25 °C). The actual pH varies from 7.0 to 6.4 as the temperature varies from 4 to 65 °C (*47*, *48*). This variation is not expected to affect P1 duplex formation or P1 docking (see the Results), and the ~4-fold variation in the chemical step from this pH change (Figure 3; *21*) does not significantly affect the results or conclusions. The curves are drawn to guide the eye and are not fits to a particular model.

by the chemical step. - -$CUCUA_5$ exhibits intermediate behavior. Between pH 5.0 and 5.8, $(k_{cat}/K_m)^S$ increases log-linearly with a slope of 1, suggesting that the reactions are limited by the chemical step. At the higher pH values (pH 5.8−7.0), $(k_{cat}/K_m)^S$ becomes independent of pH, suggesting that the chemical step is now sufficiently fast that another step becomes rate-limiting.

The interpretations described above were tested and confirmed by measuring thio effects for the shortened substrates as a function of pH. Previous results have shown that the chemical step is slowed ~2-fold upon substitution of the *pro*-R_P phosphoryl oxygen atom at the cleavage site with sulfur (*21*, *46*, *48*). No detectable thio effects were observed for reactions of -$CCUCUA_5$. In contrast, thio effects of 1.8 ± 0.3 were observed for reactions of - - -$UCUA_5$ between pH 5.6 and 7.0 (data not shown), confirming that the chemical step is rate-limiting. For - -$CUCUA_5$, a thio effect of 1.7 ± 0.1 was observed at pH 5.0 whereas the thio effects went to 1.1 ± 0.1 at the higher pH values (pH 6.2−7.0; data not shown), confirming that a step other than chemical cleavage becomes rate-limiting at higher pH. This step could be either P1 duplex formation or P1 docking. However, the rate constant for open complex formation with 5′-pyrene-labeled - -CUCU is greater than the $(k_{cat}/K_m)^S$ value for - -$CUCUA_5$ (*25*; see above). Further, the rate of duplex formation in solution is in general not significantly affected by shortening the duplex from six to three base pairs (*54*−*57*). These observations together with the results described above suggest that P1 docking and not P1 duplex formation limits $(k_{cat}/K_m)^S$ for - -$CUCUA_5$ at the higher pH values. This conclusion is supported by the temperature dependence presented in the following section.

Temperature Dependence Distinguishes Rate-Limiting P1 Duplex Formation from Rate-Limiting P1 Docking. If the reaction of E^G and unbound oligonucleotide substrate were limited by P1 duplex formation, the simplest expectation is that the rate constant of this reaction $[(k_{cat}/K_m)^S]$ would be largely invariant with respect to temperature. This is because the rate constant for duplex formation in solution exhibits a shallow temperature dependence (*54*−*58*). Figure 4 shows that this is indeed observed with the full-length substrate, $CCCUCUA_5$, and with -$CCUCUA_5$ between 10 and 60 °C, consistent with the above conclusion that P1 duplex formation is rate-limiting for these substrates.

In contrast, $(k_{cat}/K_m)^S$ for - -$CUCUA_5$ increases as the temperature is lowered, reaching a limiting value that is the same, within error, as that for $CCCUCUA_5$ and -$CCUCUA_5$ below 15 °C (Figure 4). This observation and the absence of a pH dependence above pH 5.8 (Figure 3; data not shown) suggest that $(k_{cat}/K_m)^S$ for - -$CUCUA_5$ is limited by P1 duplex formation below 15 °C and at neutral pH. The steep temperature dependence for - -$CUCUA_5$ above 30 °C suggests that P1 duplex formation does not limit the reaction rate. This result, together with the lack of a pH dependence between 5.8 and 7 (Figure 3), suggests that P1 docking limits the reaction rate for - -$CUCUA_5$ under the standard conditions (50 °C and pH 6.6). For -$CCUCUA_5$, the temperature dependence of $(k_{cat}/K_m)^S$ and the absence of a pH dependence and thio effect (data not shown) above 60 °C analogously suggests a change in the rate-limiting step from P1 duplex formation below 60 °C to P1 docking above 60 °C.

Free Energy Reaction Profiles Describing Changes in the Rate-Limiting Step. The effects of varying substrate length, pH, and temperature on the rate-limiting step are described by the reaction profiles of Figures 5−7, respectively. Each

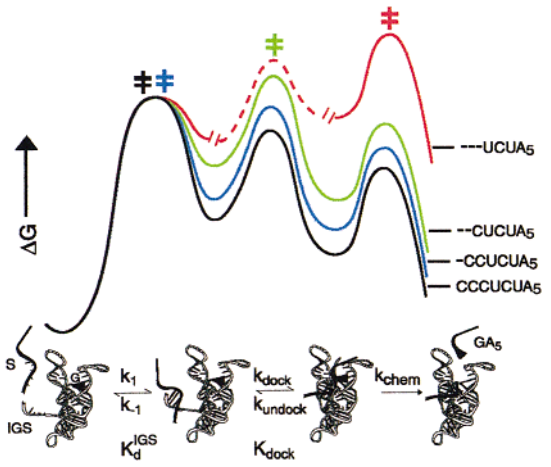

FIGURE 5: Schematic free energy profiles depicting the effect of substrate length on the identity of the rate-limiting step for the reaction $E^G + S \rightarrow$ products (50 °C, pH 6.6, and 10 mM $MgCl_2$). The free energy profiles are constructed as described in Materials and Methods. The profile for $CCCUCUA_5$ is black, for -$CCUCUA_5$ blue, for - -$CUCUA_5$ green, and for - - -$UCUA_5$ red. The highest point in a given free energy profile, "‡", is depicted in the corresponding color. The barriers for docking and undocking are not explicitly shown for - - -$UCUA_5$ as the data only establish a lower limit for these rate constants (see Materials and Methods).

reaction profile schematically depicts the free energy barriers associated with the individual reaction steps and is constructed on the basis of rate and equilibrium constants obtained here and previously (see Materials and Methods).

Figure 5 depicts reaction profiles for the full-length and shortened substrates at 50 °C and pH 6.6. Under these conditions, P1 duplex formation is rate-limiting for $CCCUCUA_5$ (Figure 5, black ‡).[2] Shortening the substrate reduces the number of base pairs in the P1 duplex and hence is expected to increase the rate constant for dissociation of the P1 duplex, k_{-1} (*54*−*57*). In contrast, the analysis in the next section suggests that shortening the substrate by two residues does not significantly affect the rate and equilibrium constants for P1 docking or the rate constant for the chemical step. For -$CCUCUA_5$, k_{-1} is larger than for $CCCUCUA_5$ (Figure 5, blue profile) but duplex dissociation remains slower than the subsequent steps (Figure 5, blue profile where $k_{-1} \ll k_{dock}$). Hence, analogous to the full-length substrate,

[2] The rate-limiting step is defined as the step that when changed causes the largest change in the overall rate of the reaction (*59*, *60*). This is illustrated for reaction conditions with subsaturating E^G and S levels in the free energy profiles of Figure 5. The rate-limiting step for reaction of - -$CUCUA_5$ (green profile) is P1 docking because changing the rate of P1 docking (k_{dock}) changes the overall rate of the reaction whereas changing the rate of P1 duplex formation (k_1) or chemical cleavage (k_{chem}) does not affect the overall rate. For subsaturating conditions, the rate-limiting step is not determined by the largest free energy barrier, which is associated with P1 duplex formation for the reaction of - -$CUCUA_5$ (Figure 5, k_1 for green profile), but rather by the highest point on the overall free energy profile, which is represented by the activation barrier for P1 docking (Figure 5, green ‡). The rate-limiting step can be distinguished between two successive steps by analyzing the partitioning of the intermediate species. For example, in the reaction profile for - -$CUCUA_5$ (Figure 5), $k_{-1} > k_{dock}$ and the open complex partitions more often to E^G and S than to the closed complex and subsequent cleavage so that the formation of the open complex represents a pre-equilibrium step and the rate is limited by P1 docking. In contrast, in the reaction profile for $CCCUCUA_5$ (Figure 5, black profile), $k_{-1} \ll k_{dock}$. In this case, essentially every time the open complex is formed it docks and is cleaved so that the rate is limited by P1 duplex formation.

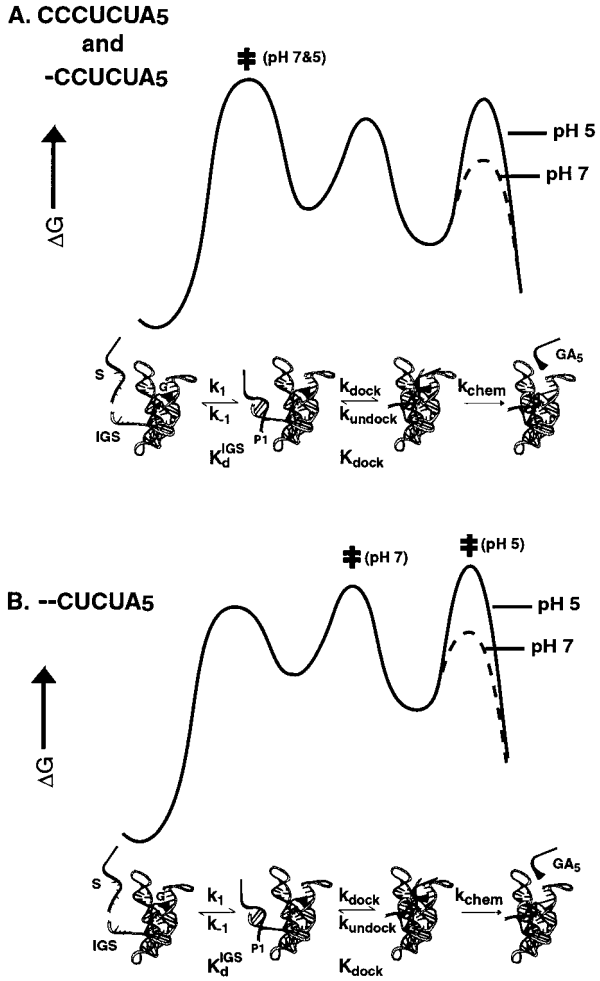

FIGURE 6: Free energy profiles depicting the effect of pH on the identity of the rate-limiting step for the reaction $E^G + S \rightarrow$ products (50 °C and 10 mM $MgCl_2$). Although there are quantitative differences in the free energy profiles for $CCCUCUA_5$ and -$CCUCUA_5$, the overall effects of varying pH are the same, so the same free energy profile is used to depict the reactions of both the substrates.

P1 duplex formation limits the reaction rate. Removal of two base-pairing residues to give - -$CUCUA_5$ sufficiently increases k_{-1} that it becomes greater than the rate constant for docking, k_{dock} (Figure 5, green profile where $k_{-1} \gg k_{dock}$ vs black profile where $k_{-1} \ll k_{dock}$). As a result, the barrier for P1 docking is now higher than that for P1 duplex dissociation (Figure 5, green ‡), and P1 docking becomes rate-limiting. Removal of three residues to give - - -$UCUA_5$ increases k_{-1} but also decreases the equilibrium constant for docking, K_{dock}, as described in the next section (Figure 5, K_{dock} for red vs black profiles). The unfavorable docking equilibrium unmasks the chemical step (Figure 5, red ‡), resulting in rate-limiting chemical cleavage.

Figure 6 depicts free energy reaction profiles for 50 °C and two pH values, 7 and 5. As described above, lowering the pH from 7 to 5 decreases the rate constant for the chemical step, k_{chem}, in a log-linear manner (*21*, *48*) but is not expected to affect the rate and equilibrium constants for P1 duplex formation and P1 docking. For the full-length substrate and for -$CCUCUA_5$, dissociation from E, which is limited by dissociation of the P1 duplex, remains slower than the chemical step even when the pH is lowered from 7 to 5. Hence, P1 duplex formation remains rate-limiting (Figure

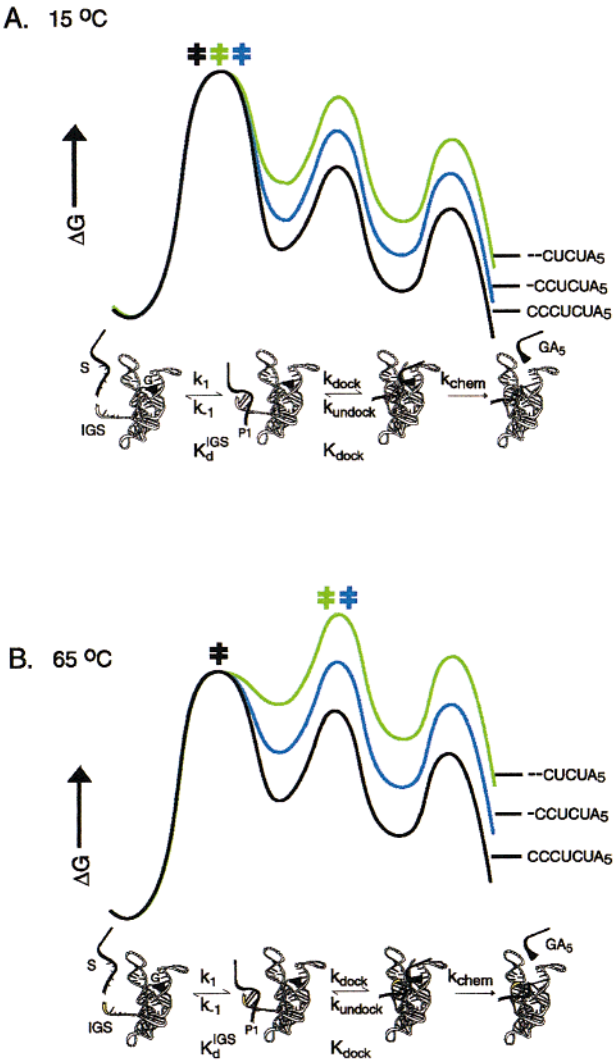

FIGURE 7: Free energy profiles depicting the effect of temperature on the identity of the rate-limiting step for the reaction $E^G + S \rightarrow$ products (pH 7 and 10 mM $MgCl_2$), as described in the legend of Figure 5.

6A, ‡). For - -CUCUA$_5$, rate-limiting P1 docking at pH 7 implies that docking is slower than P1 duplex dissociation and undocking is slower than the chemical step (Figure 6B, pH 7 where $k_{-1} \gg k_{dock}$ and $k_{undock} \ll k_{chem}$). Lowering the pH to 5 sufficiently decreases k_{chem} that k_{chem} becomes smaller than k_{undock}, rendering the chemical step rate-limiting (Figure 6B, ‡ at pH 5 vs 7).

Figure 7 compares the temperature dependencies of the free energy profiles for the full-length substrate, CCCUCUA$_5$, and for -CCUCUA$_5$ and - -CUCUA$_5$ at pH 7. For each substrate at 15 °C, dissociation of the P1 duplex is slower than the steps following P1 duplex formation (Figure 7A, $k_{-1} \ll k_{dock}$) so that P1 duplex formation is rate-limiting (Figure 7A, ‡). Raising the temperature is expected to increase the rate constant for dissociation of the P1 duplex because duplexes in solution dissociate faster at higher temperatures (*54*−*58*), whereas the analysis in the next section suggests that the rate constant for docking is largely independent of temperature. For -CCUCUA$_5$ and - -CUCUA$_5$, raising the temperature to 65 °C increases the rate constant for dissociation of the P1 duplex to the extent that it becomes faster than docking (Figure 7B, $k_{-1} \gg k_{dock}$). Hence, P1 docking limits the reaction rate of -CCUCUA$_5$ and - -CUCUA$_5$ at 65 °C (Figure 7B, blue and green ‡). The transition from rate-limiting P1 duplex formation to rate-limiting docking happens at a lower temperature for - -CUCUA$_5$ than for -CCUCUA$_5$ because the P1 duplex formed with - -CUCUA$_5$ dissociates faster than that formed with -CCUCUA$_5$. For the full-length substrate, duplex dissociation remains slower than docking at 65 °C so that the rate remains limited by P1 duplex formation (Figure 7B, black ‡).

The ability to isolate the steps of P1 duplex formation, P1 docking, and chemical cleavage by varying substrate length, pH, or temperature as illustrated above allowed us to obtain information about the nature of these individual steps, as described in the following section.

Investigating the Individual Reaction Steps: P1 Duplex Formation, P1 Docking, and Chemical Cleavage

This section analyzes the effects of substrate length, pH, and temperature on the individual reaction steps. The results of the analysis are summarized in Table 2 for reference and comparison.

Effect of Temperature, pH, and Substrate Length on the Rate Constant for P1 Duplex Formation. As described above, the absence of a pH dependence, temperature dependence, or thio effect for $(k_{cat}/K_m)^S$ with CCCUCUA$_5$ and -CCUCUA$_5$ [Figures 3 and 4 (*21*, *46*, *48*, *54*−*58*); D. S. Knitt and D. Herschlag, unpublished results] supports the assignment of rate-limiting P1 duplex formation for these substrates. Conversely, the pH and temperature effects are consistent with P1 duplex formation being largely unaffected by variations in pH and temperature. Analogously, the identical values of $(k_{cat}/K_m)^S$ for - -CUCUA$_5$ and the full-length substrate below 15 °C (Figure 4) suggest that P1 duplex formation also limits the reaction rate of - -CUCUA$_5$ at these temperatures. Together, these data provide a self-consistent picture in which the P1 duplex is formed with a rate constant of $\sim 10^8$ M^{-1} min^{-1} over the temperature and pH range investigated for duplexes 4−6 bp in length; the results provide only a lower limit of 2.9×10^4 M^{-1} min^{-1} for the rate of formation of a 3 bp P1 duplex.

Effect of Substrate Length and Temperature on the Rate Constant for P1 Docking, k_{dock}. (1) Obtaining the Rate Constant for P1 Docking, k_{dock}. For cases with rate-limiting P1 docking, k_{dock} was first deconvoluted from the overall $(k_{cat}/K_m)^S$ value. This then allowed analysis of the effects of substrate length and pH on k_{dock}.

For - -CUCUA$_5$, the observed reaction rate and the pH and temperature dependence of $(k_{cat}/K_m)^S$ suggest that P1 docking limits $(k_{cat}/K_m)^S$ between 30 and 65 °C at pH 7, as described above. Under these conditions, there is sufficient time to establish an equilibrium population of the open complex prior to rate-limiting P1 docking (Figure 5, green profile where $k_{-1} \gg k_{dock}$).[2] Hence, $(k_{cat}/K_m)^S$ is related to the equilibrium dissociation constant for the open complex, K_d^{IGS}, and k_{dock} according to eq 4 (Figure 5, green profile).

$$(k_{cat}/K_m)^S = k_{dock}/K_d^{IGS}; \quad k_{dock} = (k_{cat}/K_m)^S \times K_d^{IGS} \quad (4)$$

Table 3 lists the observed values of $(k_{cat}/K_m)^S$, the estimated values of K_d^{IGS}, and the resultant values of k_{dock}. The values of K_d^{IGS} were estimated from the binding affinity of - -CmUCUA$_5$, a substrate with a 2′-methoxy substituent at the −3 position (Figure 2B). Previous work has strongly

Table 2: Summary of the Effects of Substrate Length, pH, and Temperature on the Individual Reaction Steps[a]

	P1 duplex formation			P1 docking			chemical step
	k_1	k_{-1}	$K_a^{IGS\,b}$	k_{dock}	k_{undock}	K_{dock}	k_{chem}
shortening substrate[c]	O	+	−	O (ND for $UCUA_5$)	O (ND for $UCUA_5$)	O, −[d]	O
increasing pH[e]	O	O	O	O	O	O	+
increasing temperature[f]	O	+	−	O	−	+	+

[a] Individual rate and equilibrium constants are defined in the legend of Figure 2A: +, increase; −, decrease; O, no change; and ND, not determined. [b] $K_a^{IGS} = 1/K_d^{IGS}$. [c] pH 7 and 50 °C; from the Results. [d] K_{dock} is similar for $CCCUCUA_5$, -$CCUCUA_5$, and - -$CUCUA_5$ but is decreased for - - -$UCUA_5$ relative to those of the longer substrates (see the Results). [e] At 50 °C; from the Results and refs *21*, *41*, and *48*. [f] pH 7; from the Results and refs *23* and *49*.

Table 3: Estimation of the Rate Constant for Docking of the P1 Duplex, k_{dock}[a]

	- -$CUCUA_5$			-$CCUCUA_5$		
T (°C)	$(k_{cat}/K_m)^{S\,b}$ (M^{-1} min^{-1})	$K_d^{IGS\,c}$ (M)	k_{dock}^{d} (min^{-1})	$(k_{cat}/K_m)^{S\,b}$ (M^{-1} min^{-1})	$K_d^{IGS\,c}$ (M)	k_{dock}^{d} (min^{-1})
30	4.6×10^{7} [e]	8.9×10^{-6}	550	−	−	−
40	1.7×10^{7}	3.7×10^{-5}	630	−	−	−
50	7.1×10^{6}	1.4×10^{-4}	990	−	−	−
55	5.0×10^{6}	2.6×10^{-4}	1300	−	−	−
60	2.3×10^{6}	4.9×10^{-4}	1130	−	−	−
65	5.8×10^{5}	9.0×10^{-4}	520	1.7×10^{7}	4.2×10^{-5}	710

[a] Conditions: 50 mM NaMES, pH 6.8 (pH value at 25 °C), and 10 mM $MgCl_2$. [b] $(k_{cat}/K_m)^S$ is the second-order rate constant for the reaction $E^G + S \rightarrow$ products. Each $(k_{cat}/K_m)^S$ value is the average of the individual values depicted in Figure 4. [c] K_d^{IGS} is the equilibrium constant for dissociation of S from the open complex (Figure 2A). [d] k_{dock} was obtained using eq 4. [e] At 30 °C, $(k_{cat}/K_m)^S$ for - -$CUCUA_5$ is only 4-fold slower than for the full-length substrate, suggesting that P1 duplex formation provides a small contribution toward limiting the reaction rate. Hence, the k_{dock} value at 30 °C was obtained from the equation $(k_{cat}/K_m)^S = (k_1 k_{dock})/(k_{-1} + k_{dock})$, derived for conditions with P1 duplex formation and P1 docking being partially rate-limiting. The $(k_{cat}/K_m)^S$ value of 1.8×10^8 M^{-1} min^{-1} for the full-length substrate was used for k_1 because Figure 4 suggests that P1 duplex formation occurs at the same rate for $CCCUCUA_5$ and - -$CUCUA_5$ (see the Results). The value of k_{-1} was obtained from $k_{-1} = K_d^{IGS} k_1$ (Figure 2A).

suggested that the E·S complex formed with such substrates is a good mimic of the open complex formed with the corresponding all-RNA substrate (*39*, *49*; also see Materials and Methods). An analogous calculation of k_{dock} was possible for -$CCUCUA_5$ at 65 °C (Table 3) because, as described above, $(k_{cat}/K_m)^S$ for -$CCUCUA_5$ is limited by P1 docking at this temperature (Figure 7B, blue profile).

(2) The Rate Constant for P1 Docking Is Not Greatly Affected by Substrate Length and Temperature. The k_{dock} value of 710 min^{-1} obtained from the analysis described above for -$CCUCUA_5$ is the same, within error, as the value of 520 min^{-1} obtained for - -$CUCUA_5$ at this temperature (Table 3) (errors are estimated as ±35%; see Materials and Methods), suggesting that this change in substrate length does not substantially alter the rate of docking.

The data in Table 3 for - -$CUCUA_5$ further suggest that k_{dock} does not vary significantly with temperature. This temperature dependence was analyzed according to transition state theory. The Arrhenius plot of $\ln(k_{dock})$ versus 1/temperature gives the change in enthalpy, $\Delta H^{\ddagger}_{dock}$ (5.2 ± 10 kcal/mol), and the change in entropy, $\Delta S^{\ddagger}_{dock}$ (−37 ± 27 cal mol^{-1} K^{-1}), associated with the formation of the transition state for docking (Figure 8). The k_{dock} value at 65 °C was omitted for this analysis because the tertiary structure of the ribozyme is partially disrupted at this temperature (*30*). The error limits are highly conservative estimates and were obtained as described in Materials and Methods to determine if the sign of $\Delta S^{\ddagger}_{dock}$ can be ascribed convincingly (see the Discussion).

The $\Delta H^{\ddagger}_{dock}$ and $\Delta S^{\ddagger}_{dock}$ values obtained here are considerably different from the $\Delta H^{\ddagger}_{dock}$ value of 22 kcal/mol and $\Delta S^{\ddagger}_{dock}$ value of 21 cal mol^{-1} K^{-1} obtained previously using a 5′-pyrene-labeled - -CUCU oligonucleotide, with $\Delta S^{\ddagger}_{dock}$

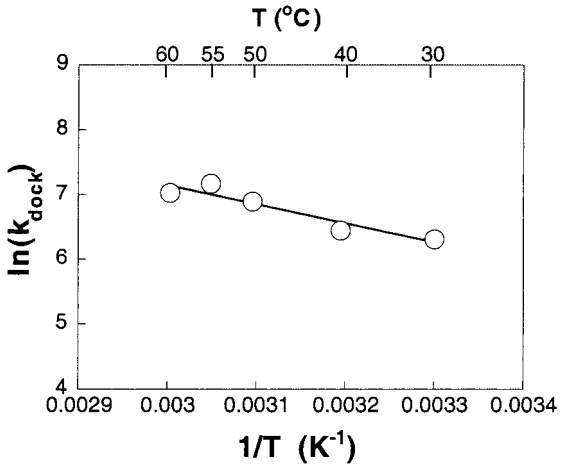

FIGURE 8: Effect of temperature on the rate constant for P1 docking, k_{dock}. The values of k_{dock} are from Table 3. The line represents a fit to the data that give a $\Delta H^{\ddagger}_{dock}$ of 5.2 ± 10 kcal/mol and a $\Delta S^{\ddagger}_{dock}$ of −37 ± 27 cal mol^{-1} K^{-1} (eq 1). The error limits are conservative estimates as described in Materials and Methods.

even differing in sign (*27*). The origin of the differences may lie in the different oligonucleotides or the different conditions used in the two studies, as described below.

(i) The activation parameters for docking of the oligonucleotide substrate, - -$CUCUA_5$, used here, may be intrinsically different from those of the oligonucleotide product, - -CUCU, used in the previous study. An effect from the 3′-extension is consistent with the previous observation that the oligonucleotide product - -pyrCUCU docks ~4-fold faster than - -pyrCUCUA (*26*). The 5′-pyrene group attached to - -CUCU in the previous study may also affect the activation parameters. (ii) The previous study used a model duplex

between - -pyrCUCU and a modified IGS strand, GGAGAA, to estimate the stability of the open complex, K_d^{IGS}, whereas here the stability of the open complex has been directly measured using substrate analogues (see Materials and Methods). Although at 15 °C, the open complex formed with - -pyrCUCU exhibits the same stability as the model duplex (*25*), possible differences at other temperatures would affect the activation parameters obtained previously. (iii) The previous experiments were carried out in the absence of G with 5 mM $MgCl_2$ and 160 mM Na^+ at pH 7.4, whereas the experiments described here were carried out using a saturating G concentration with 10 mM $MgCl_2$ and 40 mM Na^+ at pH 6.8. Binding of G has been shown to stabilize the docked state (*22*). (iv) The temperature range of 10−25 °C used in the previous study differs from the range of 30−60 °C investigated herein. Previous observations of a change in the energetic coupling between G and S binding have suggested a structural transition in the ribozyme around 30 °C (*23*). Hence, the two studies may have characterized P1 docking for distinct states of the ribozyme.

Effect of Substrate Length on the Equilibrium Constant for P1 Docking, K_{dock}. For the full-length substrate, K_{dock} was obtained from the equilibrium constant for dissociation of S from the E·S complex, K_d^E, and the equilibrium constant for dissociation of S from the open complex, K_d^{IGS}, using eq 5, which is derived from Figure 2A. The value of K_d^E was taken from previous measurements (*22, 41*), and the value of K_d^{IGS} was estimated from the binding affinity of a substrate analogue that has a 2′-methoxy substituent at the −3 position (see above and Materials and Methods).

$$K_{dock} = K_d^{IGS}/K_d^E - 1 \quad (5)$$

Shortening the substrate weakens binding, hindering a direct measurement of K_d^E. Hence, for the shortened substrates, K_{dock} was obtained indirectly using values of $(k_{cat}/K_m)^S$ under conditions of rate-limiting chemical cleavage (e.g., Figure 6B, pH 5 profile). Under these conditions, the chemical step is slower than the steps limiting dissociation of the substrate from the closed complex. Hence, there is sufficient time to establish an equilibrium population of the closed complex prior to rate-limiting chemical cleavage. The value of $(k_{cat}/K_m)^S$ then relates to K_d^{IGS}, K_{dock}, and the rate constant for the chemical step, k_{chem}, according to eq 6, which is derived from Figure 2A.

$$(k_{cat}/K_m)^S = k_{chem} \times K_{dock}/K_d^{IGS};$$
$$K_{dock} = (k_{cat}/K_m)^S \times K_d^{IGS}/k_{chem} \quad (6)$$

To obtain K_{dock} using eq 6, conditions of rate-limiting chemical cleavage were first established for the shortened substrates. As described above, under the standard conditions (pH 6.6 and 50 °C), $(k_{cat}/K_m)^S$ for - - -UCUA$_5$ is limited by the chemical step but $(k_{cat}/K_m)^S$ for -CCUCUA$_5$ and - -CUCUA$_5$ is not (Figure 3). To render the chemical step rate-limiting for the reaction of -CCUCUA$_5$ and - -CUCUA$_5$, the 2′-OH at the cleavage site was replaced with a 2′-H. This substitution slows the chemical step ∼500-fold without affecting K_{dock} (Table 4; *21, 36, 41, 52*). The log-linear pH dependence of $(k_{cat}/K_m)^S$ for -CCUC<u>dU</u>A$_5$ and - -CUC<u>dU</u>A$_5$ with a slope of 1 strongly suggests that the chemical step is indeed rate-limiting (data not shown) (*21*). As above, the K_d^{IGS} values used in eq 6 were estimated from the binding affinities of modified substrates having a 2′-methoxy substituent at the −3 position (see Materials and Methods). The k_{chem} values for the shortened substrates were assumed to be the same as that previously measured for the full-length substrate (*19, 39*), and this assumption is supported by the results listed in Table 5.

Table 4: Effect of Shortening the Substrate on K_{dock}, the Equilibrium Constant for P1 Docking[a]

substrate	$(k_{cat}/K_m)^S$ [b] (M^{-1} min^{-1})	K_d^{IGS} [c] (M^{-1})	k_{chem} [d] (min^{-1})	K_{dock} [e]	K_{dock}^{rel} [f]
CCCUC<u>dU</u>A$_5$	−	2.1×10^{-7}	0.3	63[g]	(1)
-CCUC<u>dU</u>A$_5$	3.9×10^6	6.9×10^{-6}	0.3	90[h]	1.4
- -CUC<u>dU</u>A$_5$	2.4×10^4	4.2×10^{-4}	0.3	34[h]	0.5
CCCUC<u>U</u>A$_5$	−	7.0×10^{-8}	200	63[g]	(1)
- - -UCUA$_5$	2.9×10^4	2.0×10^{-3}	200	0.3[h]	0.005

[a] Conditions: 50 °C, 50 mM sodium MES, pH 6.6, and 10 mM $MgCl_2$. [b] $(k_{cat}/K_m)^S$ is the second-order rate constant for the reaction $E^G + S \rightarrow$ products. [c] K_d^{IGS} is the equilibrium constant for dissociation of S from the open complex. [d] k_{chem} is the rate constant for the chemical step (Figure 2A). The k_{chem} value for the full-length substrate is used for the shortened substrates because at 10 °C all the substrates have similar k_{chem} values (see Table 5 and the Results); the value of k_{chem} for CCCUC<u>dU</u>A$_5$ was measured as described in Materials and Methods, and the value of k_{chem} for CCCUCUA$_5$ was taken from previous estimates (*19, 21, 39*). [e] K_{dock} is the equilibrium constant for P1 docking (Figure 2A). [f] A K_{dock}^{rel} of <1 indicates a destabilizing effect of shortening the substrate: $K_{dock}^{rel} = K_{dock}^{(shortened-S)}/K_{dock}^{(full-length-S)}$. [g] Obtained from eq 5 as described in the Results using K_d^E values of 1.1×10^{-9} and 3.1×10^{-9} M for CCCUCUA$_5$ and CCCUC<u>dU</u>A$_5$, respectively. These values were obtained from the previously measured K_d^E values of 8×10^{-9} and 2.2×10^{-8} M for CCCUCUA$_5$ and CCCUC<u>dU</u>A$_5$, respectively, with a subsaturating G concentration and the 7-fold stabilizing effect of bound G on the binding of these substrates [$K_d^E = K_d^{E(subsaturating-G)}/7$ (*22, 41*)]. [h] Obtained from $(k_{cat}/K_m)^S$, K_d^{IGS}, and k_{chem} using eq 6 as described in the Results.

Table 5: Comparison of k_{chem} Values for Full-Length and Shortened Substrates[a]

substrate	pH	k_{chem} (min^{-1})[b]	substrate	pH	k_{chem} (min^{-1})[b]
CCCUCUA$_5$	5.4	0.13	CCCUCUA$_5$	6.3	1.0
-CCUCUA$_5$	5.4	0.10	- - -UCUA$_5$	6.3	0.3[c]
- -CUCUA$_5$	5.4	0.16			

[a] Conditions: 10 °C and 10 mM $MgCl_2$. [b] k_{chem} is the rate constant for the reaction from the $(E^G \cdot S)_{closed}$ complex and was obtained as described in Materials and Methods. [c] k_{chem} for - - -UCUA$_5$ is a lower limit as described in the Results.

The values of K_{dock} for the shortened substrates obtained using eq 6 and the value of K_{dock} for the full-length substrate obtained from eq 5 are summarized in Table 4. The results suggest that K_{dock} is the same, within error, for CCCUC<u>dU</u>A$_5$, -CCUC<u>dU</u>A$_5$, and - -CUC<u>dU</u>A$_5$. In contrast, the value of K_{dock} for - - -UCUA$_5$ is ∼200-fold smaller than that for CCCUCUA$_5$.

Effect of Substrate Length on the Rate Constant for the Chemical Step, k_{chem}. The value of k_{chem} was obtained from the rate constant for the reaction of the $E^G \cdot S$ ternary complex under conditions for which the substrate is predominantly docked (Figure 2A, k_{chem}). The rate constants were measured at 10 °C to allow saturation with the shorter substrates. At 10 °C, binding of the full-length substrate to an 5′-azidophenacyl-labeled ribozyme gives a site-specific cross-link, the location of which is indicative of a docked P1 duplex (*14, 15*; G. J. Narlikar and D. Herschlag, unpublished results).

Further, - -CUCUA$_5$ binds to E^G ~20-fold more strongly at 10 °C than a substrate analogue that binds predominantly in the open complex (G. J. Narlikar and D. Herschlag, unpublished results), suggesting that - -CUCUA$_5$ is predominantly docked. Together, these results suggest that the E^G•S ternary complex formed with - -CUCUA$_5$ and longer oligonucleotide substrates at 10 °C represents the closed complex. For - - -UCUA$_5$, there is no direct evidence that the E^G•S ternary complex is in the closed complex at 10 °C, so the k_{chem} value obtained below is a lower limit.

For - -CUCUA$_5$ and -CCUCUA$_5$, saturation could be achieved using excess E over S. Binding of - - -UCUA$_5$ is still too weak at 10 °C to achieve saturation using excess E, and so its k_{chem} value was estimated from the k_{cat} value obtained using excess - - -UCUA$_5$ over E. The pH was lowered to 5.4 or 6.3 to facilitate measurement of the chemical step, which is faster than can be reliably measured by manual pipetting at pH 7 (*23*). The results are summarized in Table 5. At 10 °C, the rate constant for the reaction of the E^G•S ternary complex is the same, within error, for CCCUCUA$_5$, -CCUCUA$_5$, and - -CUCUA$_5$ and is only ~3-fold smaller for - - -UCUA$_5$ than for CCCUCUA$_5$. These results suggest that the rate of the chemical step is largely unaffected by variations in substrate length and that all the substrates, including - - -UCUA$_5$, are docked or nearly docked. If a substrate was predominantly undocked, it would have been expected to react substantially slower than the full-length substrate because of an additional energetic barrier for P1 docking.

DISCUSSION

Binding of the *Tetrahymena* ribozyme's oligonucleotide substrate presents an opportunity to investigate a local RNA folding event in which secondary and tertiary folding occur in two distinct steps, P1 duplex formation and P1 docking (Figure 2) (*12*, *14*, *15*, *20*, *24*, *25*, *34*−*41*). Here we have identified reaction conditions under which P1 duplex formation, P1 docking, or the chemical step is rate-limiting. This has facilitated characterization of the individual steps and provided insights into the nature of P1 duplex formation and P1 docking as discussed below.

The Open Complex Behaves in a Manner Similar, but Not Identical, to That of a Simple Duplex. Initial work with mutant ribozymes demonstrated that the oligonucleotide substrate could move from one tertiary binding register to another without dissociating from the ribozyme (*20*). This led to a two-step model for substrate binding in which initial duplex (P1) formation between the substrate and the IGS to give an open complex was followed by docking of the duplex into tertiary interactions. It was further shown that the stabilities of transiently formed or thermodynamically stable open complexes are the same, within error, as the stabilities of model duplexes in solution, supporting the above description of the open complex (*25*, *49*; Figure 2A). The data here suggest that the rate of open complex formation is largely independent of substrate length, pH, and temperature, also analogous to duplex formation in solution. These results extend the analogy between the open complex and a duplex in solution.

Nevertheless, there are differences between the open complex and a model duplex. The rate constants for formation and dissociation of the P1 duplex are at least 10-fold smaller than the corresponding rate constants for a model duplex (*25*, *41*). The slower rates could arise if steric constraints imposed by regions of the ribozyme near the IGS restrict the conformational freedom and accessibility of the IGS relative to an oligonucleotide in solution (*61*). This would limit the number of ways in which the oligonucleotide substrate could approach toward or depart from the IGS. Indeed, the rate of P1 duplex formation increases with increasing Mg^{2+} concentration, suggesting that binding of Mg^{2+} increases the accessibility of the IGS, overcomes an electrostatic repulsion, or provides an electrostatic attraction for oligonucleotides (*62*, *63*). Further, an azidophenacyl group attached at the 5′-end of the IGS makes site-specific cross-links with peripheral regions of the ribozyme in the absence of substrate and with oligonucleotides that bind predominantly in the open complex (*14*, *15*, *49*). This is consistent with conformational restriction of the free IGS and the P1 duplex in the open complex.

In summary, the results described above suggest that the open complex can be approximated by a model duplex, but that some differences arise from differences between the ribozyme and solution environments. Analogous to the importance of characterizing the unfolded states of proteins (*64*−*67*), further characterization of the nature of the open complex will be important in better understanding the tertiary folding process of P1 docking.

The Transition State for P1 Docking Does Not Resemble the Closed Complex. The results discussed above suggest that only base pairing interactions are formed in the open complex. Hence, the step of P1 docking approximates a simple tertiary folding event in which a single duplex adopts its final tertiary structure. In previous work, a temperature dependence of the equilibrium constant for P1 docking was carried out to characterize this tertiary folding step (*27*, *49*). The results suggested that formation of the closed complex is accompanied by a gain in entropy ($\Delta S^{\circ\prime} = 62$ cal mol^{-1} K^{-1}). The increase in entropy can be accounted for by a model that invokes the release of bound water molecules, by structural rearrangements of the core after formation of tertiary interactions, or by a change in the number and position of metal ions bound to the ribozyme, as discussed previously (*27*, *49*).

Here, we have determined the temperature dependence of the rate constant for P1 docking, k_{dock}, to probe the nature of the transition state for docking. The results suggest that formation of the transition state is accompanied by a loss in entropy ($\Delta S^{\ddagger}_{dock} = -37 \pm 27$ cal mol^{-1} K^{-1}). The negative value of $\Delta S^{\ddagger}_{dock}$ contrasted with the positive value of $\Delta S^{\circ\prime}$ for formation of the closed complex most simply suggests that the transition state for docking does not closely resemble the final docked state. In contrast, $\Delta S^{\ddagger}$ and $\Delta S^{\circ\prime}$ are both negative for the folding of chymotrypsin inhibitor 2 and cold-shock protein CspB, and independent results suggest that the transition states for these proteins resemble the final folded state more than they resemble the unfolded state (*68*, *69*). For the ribozyme, the negative value of $\Delta S^{\ddagger}_{dock}$ could arise if all or most of the tertiary interactions are not made in the transition state.

P1 Duplex Rigidity Contributes to Stabilizing the Closed Complex. The effects of substrate length on the equilibrium constant for P1 docking, K_{dock}, underscore the role of duplex

rigidity in stabilizing tertiary structure. Shortening the substrate by three residues to give - - -$UCUA_5$ reduces K_{dock} 200-fold. One model that accounts for this destabilization entails disruption of the tertiary interaction made by the 2′-OH of G25 (Figure 2B) because the base pair with G25 is broken in the P1 duplex formed with - - -$UCUA_5$. However, the observation that the 2′-OH of G25 contributes the same amount of tertiary stabilization with - - -$UCUA_5$ and CCCU-CUA_5 is inconsistent with this model (G. J. Narlikar, L. E. Bartley, and D. Herschlag, manuscript in preparation). Instead, the weaker docking of - - -$UCUA_5$ may arise from the decreased rigidity of the P1 duplex formed with - - -$UCUA_5$, which has three unpaired IGS residues and only three base pairs. The unpaired residues are expected to increase the flexibility of the P1 duplex in the open complex and thereby increase the energetic cost of docking this duplex relative to the P1 duplex with all six base pairs. Further analysis along with additional results will be presented in a future manuscript (G. J. Narlikar, L. E. Bartley, and D. Herschlag, in preparation).

The Catalytic Structure of the Closed Complex Is Not Affected by Shortening the Substrate. Once - - -$UCUA_5$ docks, it is cleaved with a rate similar to that of the full-length substrate (Table 5). Thus, although the P1 duplex formed with - - -$UCUA_5$ has increased flexibility, the available tertiary interactions appear to be sufficient to position the duplex with respect to the catalytic groups.

P1 Docking Appears To Be the Fastest Step in the Overall Tertiary Folding of the Ribozyme. Substantial previous work has suggested that the overall tertiary folding of the ribozyme entails multiple steps, with each step resulting in the formation of stable substructures (*9*, *10*, *15*, *30*−*33*). Figure 1 depicts the postulated individual tertiary folding steps,[3] along with the rate constant for each step.

The rate constant for P1 docking into its tertiary interactions with the ribozyme core was previously measured by Turner and co-workers between 10 and 25 °C using 5 mM $MgCl_2$ [k_{dock} = 540 min^{-1} for - -pyrCUCU at 25 °C (*25*−*27*)]. Here, a similar rate constant for docking was obtained under conditions closer to those used previously for studying the overall folding of the ribozyme (40 °C and 10 mM $MgCl_2$; k_{dock} = 630 min^{-1} for - -$CUCUA_5$). The results suggest that P1 docking is the fastest known step in the overall folding of the ribozyme (Figure 1). Nevertheless, it is unlikely to precede P4−P6 or P3−P7 formation because folding of P4−P6 and P3−P7 provides the core into which the P1 duplex docks. Indeed, the rate of overall tertiary folding is the same in the presence and absence of the P1 duplex, consistent with an ordered folding pathway in which P1 docks after folding of the rest of the ribozyme (R. Russell and D. Herschlag, unpublished results).

Why are the other folding steps slower than P1 docking? P1 docking involves a smaller loss of conformational entropy and thus may have a smaller activation energy barrier relative to the preceding folding steps. In addition, tertiary folding can be slowed by the formation of stable non-native interactions that have to be broken prior to correct folding (*70*, *71*). The folding of P5abc, P4−P6, and to some extent P3−P7 occurs in the context of a largely unfolded ribozyme, and hence, large regions of the ribozyme's secondary structure are available for making fortuitous non-native interactions. In contrast, P1 docking involves rearrangement of a single duplex in the context of an otherwise set ribozyme structure. This may limit the opportunities for forming non-native interactions.

Nevertheless, P1 docking, which occurs on the millisecond time scale, is still substantially slower than simpler intramolecular folding events such as hairpin formation. RNA hairpin formation takes place on a microsecond time scale (*72*), the time scale calculated for diffusion-limited end to end contact formation in a 10-residue nucleic acid (*73*). The slower rate of P1 docking compared to that of hairpin formation suggests that docking is more complex than a simple diffusional search for interacting partners. Docking may proceed via multiple substeps involving an additional conformational change, rearrangement of metal ions or water molecules, and disruption of non-native interactions, and may also require that electrostatic barriers be overcome.

[3] Here the word "step" denotes macroscopic structural rearrangements that can be experimentally resolved such as those depicted in Figure 1; each step is expected to consist of many substeps that involve small-scale structural changes and solvent rearrangements.

ACKNOWLEDGMENT

We thank members of the Herschlag laboratory for helpful comments and Leonid Beigelman for advice on thio substrate purification.

REFERENCES

1. Cech, T. R. (1988) *Gene 73*, 259−271.
2. Michel, F., and Westhof, E. (1990) *J. Mol. Biol. 216*, 585−610.
3. Lehnert, V., Jaeger, L., Michel, F., and Westhof, E. (1996) *Chem. Biol. 3*, 993−1009.
4. Downs, W. D., and Cech, T. R. (1990) *Biochemistry 29*, 5605−5613.
5. Inoue, T., and Cech, T. R. (1985) *Proc. Natl. Acad. Sci. U.S.A. 82*, 648−652.
6. Jaeger, J. A., Zuker, M., and Turner, D. H. (1990) *Biochemistry 29*, 10147−10158.
7. Jaeger, L., Michel, F., and Westhof, E. (1994) *J. Mol. Biol. 236*, 1271−1276.
8. Latham, J. A., and Cech, T. R. (1989) *Science 245*, 276−282.
9. Celander, D. W., and Cech, T. R. (1991) *Science 251*, 401−407.
10. Murphy, F. L., and Cech, T. R. (1993) *Biochemistry 32*, 5291−5300.
11. Murphy, F. L., and Cech, T. R. (1994) *J. Mol. Biol. 236*, 49−63.
12. Pyle, A. M., Murphy, F. L., and Cech, T. R. (1992) *Nature 358*, 123−128.
13. Wang, J.-F., and Cech, T. R. (1992) *Science 256*, 526−529.
14. Wang, J.-F., Downs, W. D., and Cech, T. R. (1993) *Science 260*, 504−508.
15. Wang, J.-F., and Cech, T. R. (1994) *J. Am. Chem. Soc. 116*, 4178−4182.
16. Cate, J. H., Gooding, A. R., Podell, E., Zhou, K., Golden, B. L., Kundrot, C. E., Cech, T. R., and Doudna, J. A. (1996) *Science 273*, 1678−1685.
17. Cate, J. H., Gooding, A. R., Podell, E., Zhou, K., Golden, B. L., Szewczak, A. A., Kundrot, C. E., Cech, T. R., and Doudna, J. A. (1996) *Science 273*, 1696−1699.
18. Golden, B. L., Gooding, A. R., Podell, E. R., and Cech, T. R. (1998) *Science 282*, 259−264.
19. Herschlag, D., and Cech, T. R. (1990) *Biochemistry 29*, 10159−10171.
20. Herschlag, D. (1992) *Biochemistry 31*, 1386−1399.
21. Herschlag, D., and Khosla, M. (1994) *Biochemistry 33*, 5291−5297.

22. McConnell, T. S., Cech, T. R., and Herschlag, D. (1993) *Proc. Natl. Acad. Sci. U.S.A. 90*, 8362−8366.
23. McConnell, T. S., and Cech, T. R. (1995) *Biochemistry 34*, 4056−4067.
24. Bevilacqua, P. C., and Turner, D. H. (1991) *Biochemistry 30*, 10632−10640.
25. Bevilacqua, P. C., Kierzek, R., Johnson, K. A., and Turner, D. H. (1992) *Science 258*, 1355−1358.
26. Bevilacqua, P. C., Li, Y., and Turner, D. H. (1994) *Biochemistry 33*, 11340−11348.
27. Li, Y., Bevilacqua, P. C., Mathews, D., and Turner, D. H. (1995) *Biochemistry 34*, 14394−14399.
28. Narlikar, G. J., and Herschlag, D. (1997) *Annu. Rev. Biochem. 66*, 19−59.
29. Cech, T. R., and Herschlag, D. (1996) in *Nucleic Acids and Molecular Biology* (Eckstein, F., and Lilley, D. M. J., Eds.) pp 1−17, Springer-Verlag, Berlin.
30. Banerjee, A. R., Jaeger, J. A., and Turner, D. H. (1993) *Biochemistry 32*, 153−163.
31. Laggerbauer, B., Murphy, F. L., and Cech, T. R. (1994) *EMBO J. 13*, 2669−2676.
32. Zarrinkar, P. P., and Williamson, J. R. (1994) *Science 265*, 918−924.
33. Sclavi, B., Sullivan, M., Chance, M. R., Brenowitz, M., and Woodson, S. A. (1998) *Science 279*, 1940−1943.
34. Sugimoto, N., Sasaki, M., Kierzek, R., and Turner, D. H. (1989) *Chem. Lett.*, 2223−2226.
35. Pyle, A. M., and Cech, T. R. (1991) *Nature 350*, 628−631.
36. Herschlag, D., Eckstein, F., and Cech, T. R. (1993) *Biochemistry 32*, 8299−8311.
37. Strobel, S. A., and Cech, T. R. (1993) *Biochemistry 32*, 13593−13604.
38. Pyle, A. M., Moran, S., Strobel, S. A., Chapman, T., Turner, D. H., and Cech, T. R. (1994) *Biochemistry 33*, 13856−13863.
39. Knitt, D. S., Narlikar, G. J., and Herschlag, D. (1994) *Biochemistry 33*, 13864−13879.
40. Strobel, S. A., and Cech, T. R. (1995) *Science 267*, 675−679.
41. Narlikar, G. J., Khosla, M., Usman, N., and Herschlag, D. (1997) *Biochemistry 36*, 2465−2477.
42. Zaug, A. J., Grosshans, C. A., and Cech, T. R. (1988) *Biochemistry 27*, 8924−8931.
43. Scaringe, S. A., Francklyn, C., and Usman, N. (1990) *Nucleic Acids Res. 18*, 5433−5441.
44. Rajagopal, J., Doudna, J. A., and Szostak, J. W. (1989) *Science 244*, 692−694.
45. McSwiggen, J. A., and Cech, T. R. (1989) *Science 244*, 679.
46. Herschlag, D., Piccirilli, J. A., and Cech, T. R. (1991) *Biochemistry 30*, 4844−4854.
47. Good, N. E., Winget, G. D., Winter, W., Connolly, T. N., Izawa, S., and Singh, R. M. M. (1966) *Biochemistry 5*, 467−477.
48. Knitt, D. S., and Herschlag, D. (1996) *Biochemistry 35*, 1560−1570.
49. Narlikar, G. J., and Herschlag, D. (1996) *Nat. Struct. Biol. 3*, 701−710.
50. Serra, M. J., and Turner, D. H. (1995) *Methods Enzymol. 259*, 242−261.
51. Sugimoto, N., Nakano, S., Katoh, M., Matsumura, A., Nakamuta, H., Ohmichi, T., Yoneyama, M., and Sasaki, M. (1995) *Biochemistry 34*, 11211−11216.
52. Herschlag, D., Eckstein, F., and Cech, T. R. (1993) *Biochemistry 32*, 8312−8321.
53. Young, B., Herschlag, D., and Cech, T. R. (1991) *Cell 67*, 1007−1019.
54. Porschke, D., and Eigen, M. (1971) *J. Mol. Biol. 62*, 361−381.
55. Craig, M. E., Crothers, D. M., and Doty, P. (1971) *J. Mol. Biol. 62*, 383−401.
56. Porschke, D., Uhlenbeck, O. C., and Martin, F. H. (1973) *Biopolymers 12*, 1313−1335.
57. Ravetch, J., Gralla, J., and Crothers, D. M. (1974) *Nucleic Acids Res. 1*, 109−127.
58. Nelson, J. W., and Tinoco, I., Jr. (1982) *Biochemistry 21*, 5289−5295.
59. Jencks, W. P. (1987) *Catalysis in Chemistry and Enzymology*, Dover, New York.
60. Ray, W. J., Jr. (1983) *Biochemistry 22*, 4625−4637.
61. Russell, R., and Herschlag, D. (1999) *RNA 5*, 158−166.
62. McConnell, T. S., Herschlag, D., and Cech, T. R. (1997) *Biochemistry 36*, 8293−8303.
63. Williams, A. P., Longfellow, C. E., Freier, S. M., Kierzek, R., and Turner, D. H. (1989) *Biochemistry 28*, 4283−4291.
64. Dill, K. A., and Shortle, D. (1991) *Annu. Rev. Biochem. 60*, 795−825.
65. Wrabl, J. O., and Shortle, D. (1996) *Protein Sci. 5*, 2343−2352.
66. Shortle, D. (1996) *FASEB J. 10*, 27−34.
67. Shortle, D. R. (1996) *Curr. Opin. Struct. Biol. 6*, 24−30.
68. Jackson, S. E., and Fersht, A. R. (1991) *Biochemistry 30*, 10436−10443.
69. Schindler, T., and Schmid, F. X. (1996) *Biochemistry 35*, 16833−16842.
70. Treiber, D. K., Rook, M. S., Zarrinkar, P. P., and Williamson, J. R. (1998) *Science 279*, 1943−1946.
71. Pan, T., Fang, X., and Sosnick, T. (1999) *J. Mol. Biol. 286*, 721−731.
72. Turner, D. H., Sugimoto, N., and Freier, S. M. (1990) in *Nucleic Acids* (Saenger, W., Ed.) pp 201−227, Springer-Verlag, Berlin.
73. Szabo, A., Schulten, K., and Schulten, Z. (1980) *J. Chem. Phys. 72*, 4350−4357.
74. Strobel, S. A., and Cech, T. R. (1994) *Nat. Struct. Biol. 1*, 13−17.

BI9914309